

Correlation Between Speeds of CMEs and the Intensity of Geomagnetic Storms

Vasyl Yurchyshyn¹, Haimin Wang¹, Valentyna Abramenko^{1,2}

¹Big Bear Solar Observatory, 40386 North Shore Lane, Big Bear City, CA 92314, USA

²Crimean Astrophysical Observatory, 98409, Nauchny, Crimea, Ukraine

Abstract.

We studied the relationship between the projected speed of CMEs, determined from a sequence SOHO/LASCO images, and the hourly averaged magnitude of the B_z component of the magnetic field in an interplanetary ejecta, as measured by the ACE magnetometer in the GSM coordinate system. For CMEs, that originate at the central part of the solar disk, we found that the intensity of B_z is correlated with the projected speed of the CME, V_p . The relationship is more pronounced for very fast ejecta ($V_p > 1200$ km/s), while slower events display larger scatter. We also present data which support earlier conclusions about the correlation of B_z and the Dst index of geomagnetic activity. A possible application of the results to space weather forecasting is discussed.

1. Introduction

Geomagnetic storms are major disturbances in the earth's magnetosphere that occur when the interplanetary magnetic field (IMF) turns southward and remains so for a prolonged period of time [Rostoker and Fälthammar, 1967; Russell et al., 1974]. Shortly after solar coronal mass ejections (CMEs) were discovered [Tousey, 1973; MacQueen et al., 1974; Gosling et al., 1974], it was found that the occurrence of geomagnetic storms is correlated with the occurrence of CMEs [Burlaga et al., 1981; Wilson and Hildner, 1983].

Reconnection between the southwardly directed component of the solar wind magnetic field, B_z , and the northwardly directed geomagnetic field occurs at the day side magnetopause and this reconnection transports energy from the solar wind into the magnetosphere. During a storm, the enhanced ring current is created and it greatly impacts structure of magnetospheric regions, which, in turn, results in a significant electric potential on conductors in all kinds of operating systems. As more advanced and interconnected systems are employed, the effects of the upper atmosphere become more profound. Although most operational systems can resist the effect of certain levels of geomagnetospheric activity, large storms can still cause significant damage to space- and ground-based installations, such as satellites, long-line communication networks and electric power grids. Severe geomagnetic storms occur when the IMF imposes long periods (several hours or more) of the southward component ($B_z < 0$) with large magnitudes (greater than 10–15 nT). This southward IMF stresses the earth magnetic field and the degree of this stress, the Dst index, is the measure of the intensity of the geomagnetic storm. The Dst index represents the hourly average of the deviations of the horizontal component of

the magnetic field measured by several ground stations located between mid and low-latitudes. The reference level is set so that Dst is statistically zero on internationally designated quiet days. When the Dst index varies around zero, then it is said that the geomagnetic field behaves quietly, while $Dst \leq -100$ nT means large storms.

CMEs are the result of a large-scale rearrangement of the solar magnetic field (see Low [2001] for a review) and they are often observed as an eruption of twisted magnetic fields from the solar atmosphere (Canfield et al., 1999). When the CME's source region is located near the center of the solar disk, then the CME is directed toward the earth and is normally seen, in coronagraphs, as an expanding faint halo around the sun [Howard et al. 1982]. Only those earth-directed CMEs, where the magnetic field has a southward component, are capable of producing large geomagnetic storms [Russell et al., 1974; Gonzalez et al., 1994; Cane et al., 2000; Pevtsov and Canfield, 2001].

In general, the parameters of the solar wind determine the severity of a geomagnetic storm. Burton et al. [1975] published a formula to predict the Dst index, which uses the velocity and density of the solar wind as well as the B_z component of the IMF in the GSM system, as inputs. This formula was later improved by Ferrich and Luhmann [1998]. Gonzalez and Tsurutani [1987] pointed out a relation between the Dst index and the strength of the IMF, which produced the geomagnetic disturbance: intense storms ($Dst \leq -100$ nT) were caused by large southwardly directed magnetic fields, where $B_z < -10$ nT. Later Cane et al. [2000] studied 83 events from 1996 to 1999 and found a high correlation (0.74) between the intensity of the southwardly directed IMF, B_z , and the Dst index. Recently, Wu and Lepping [2002] used hourly averaged OMNI data for 135 events from 1965 to 1998 and they found the correlation to be 0.86.

The strength of the magnetic field of an interplanetary CME (ICME) is determined by condition of the erupted solar magnetic fields as well as by compression at the front edge of an ICME during its travel through interplanetary space. While it is not clear how the magnitude of the magnetic field in a CME is related to its speed, the compression is expected to be related to the faster speed of the ICME relative to the solar wind. Indeed, Lindsay et al. [1999] reported on a possible relationship between the speed of CMEs and the magnitude of the total IMF in the associated ICMEs.

Major acceleration of fast CMEs takes place in the solar corona below 30 solar radii ($R \leq 30R_\odot$) where they reach their maximum travel speed [Sheeley et al., 1999; Shanmugaraju et al., 2003]. Cane et al. [2000] noted that the projected speed of CMEs (the expansion speed or the speed in the plane of the sky) is in direct relationship to their travel speed. Schwenn et al. [2001] also found a relationship between the CME's projected and travel speeds. According to their study, the travel speed $V = 0.88V_p$, where V_p denotes the projected speed of the CME. This implies that some correlation might exist between the projected speed and the intensity of the southward magnetic field at the leading edge of an ICME. In the present study, we examine the relationship between

the projected speed of CMEs, V_p , determined from a sequence of SOHO/LASCO images, and the strength of the southwardly directed magnetic field in ICME, B_z , by analyzing data for 14 events. The data used in this study is described in second section, while the results are presented in the third section of the paper. In the fourth section we discuss a possible application of the results to the prediction of space weather.

2. Data

We used the CME Catalog, from the Center for Solar Physics and Space Weather of The Catholic University of America (http://cdaw.gsfc.nasa.gov/CME_list/), which provided us with information on CMEs. For each of the event, the catalog contains LASCO C2 appearance time, central position angle, angular width, height-time plots with linear and 2nd order fits and acceleration. It also contains speed from linear fit to the height-time measurements, speed at the last height of measurement using quadratic fit, speed at $20R_\odot$ using quadratic fit, acceleration obtained from the quadratic fit, and the actual position angle at which the height-time measurements are made. The height of a CME was measured at the fastest segment of the ejecta. The error in the height measurements for an ejecta with a well-pronounced leading edge does not exceed 5%, while in the case of an irregular and faint edge the error increases up to 20%. The catalog speeds determined from a linear fit to the height-time profile for each event were used in our study as the projected speed of CMEs, V_p .

To locate the source region where an ejecta was originated, we used global full disk $H\alpha$ network observations, SOHO/EIT 195\AA and C2 and C3 LASCO images.

The ACE level 2 data were used to identify ICMEs and to determine the hourly averaged extremum values of the B_z component of the IMF measured in the GSM system at the front edge of the interplanetary ejecta (hereafter referred as the B_z component of the IMF). In the case when the ICME structure included both a sheath and a magnetic cloud, the maximum value of the magnetic field in the sheath was taken, otherwise, the value of the magnetic field at the front edge of a magnetic cloud was used. Events which are magnetic clouds are marked with “C” in Table I.

The intensities of geomagnetic storms were determined by hourly equatorial Dst values from the World Data Center for Geomagnetism in Kyoto. For geomagnetic storms, which occurred in 1999-2000, we used the final data whereas for geomagnetic storms in 2001 we used provisional values.

3. Correlation of the projected speed of halo CMEs and the B_z component of the IMF

To study the relationship between the projected speed of halo CMEs and the magnitude of the B_z component of the IMF we selected 14 pairs of events (CME-ICME) from 1999 to 2001. In Table I we list the selected events and include the following information about each of them: date and time of the first appearance of the CME in LASCO C2 field of view; the CME’s projected speed, V_p ; date, time and day of year when B_z in the corresponding ICME was measured; the intensity of the B_z component at the leading edge of an interplanetary ejecta.

The number of the events considered is very limited due to the following strict criteria we used to select the data: 1) the geomagnetic storm should have the associated Dst index below -50 nT and should not overlap with the recovery phase of a previous storm; 2) an interplanetary ejecta, associated with the storm, can be identified in the ACE data; 3) a full halo CME, associated with an ejecta, can be clearly seen in LASCO data; 4) a LASCO movie for each

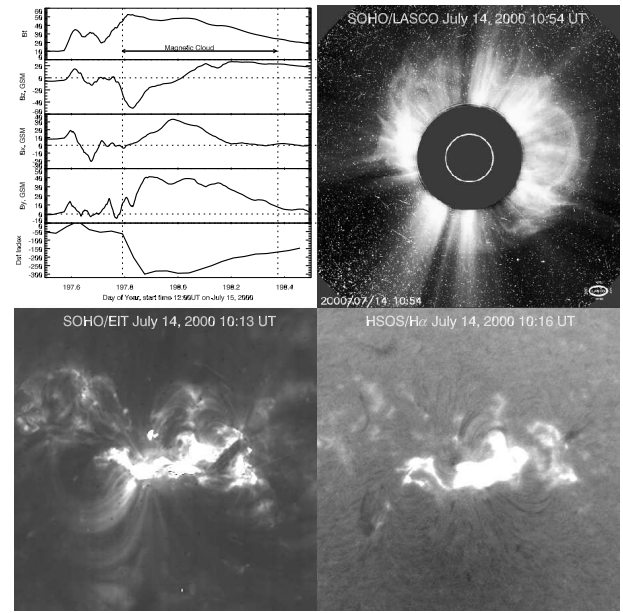


Figure 1. A typical data set used in the study. Top left panel shows ACE geomagnetic measurements (top 4 plots) and the Dst index for the July 15, 2000 geomagnetic event. Top right image shows the related coronal mass ejection as it was seen in the SOHO/LASCO C2 field of view on July 14, 2000. This ejecta was associated with the X-class “Bastille Day” flare observed with the SOHO/EIT 195\AA (bottom left panel) and the Huairou $H\alpha$ (HSOS, China) telescopes.

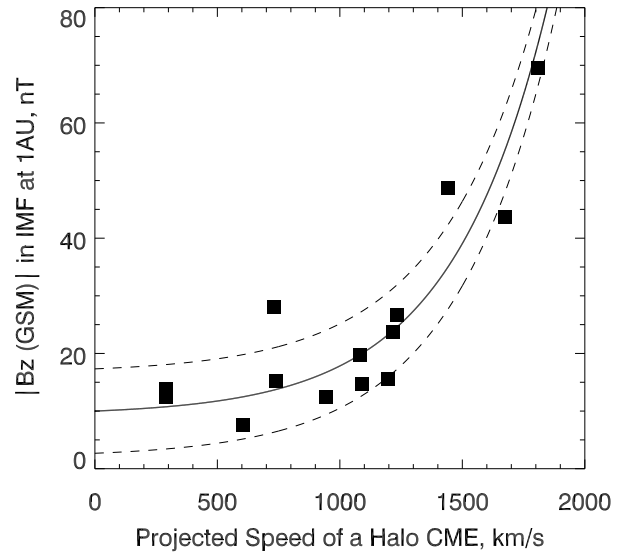


Figure 2. The absolute value the B_z component of the IMF at the leading edge of an ejecta vs. the projected speed of a CME, V_p . The solid line is an exponential fit. The dashed lines show the extent of the error to this fit.

CME is available; 5) the projected speed of the CME can be reliably determined; 6) the CME’s source region can clearly be identified in SOHO/EIT and/or $H\alpha$ images; and 7) the CME’s source region is located within 55° ($R < 0.8R_\odot$) of the central meridian (R denotes the distance from the disk center to the CME’s source region in fractions of solar radius). For each pair of events we determined the magnitude of B_z at the front edge of an ejecta. Due

to scarce number of events satisfying all the above requirements, we included three events with large northwardly directed magnetic fields (positive) regardless of the associated geomagnetic activity.

Figure 1 shows a typical data set we have compiled for each event. The top left panel displays geomagnetic data as measured by the ACE magnetometer and the Dst index during the July 15, 2000 event. The vertical dashed lines mark the beginning and the end of a magnetic cloud in the interplanetary ejecta as determined by the MFI team by using WIND data (http://lep.mfi.gsfc.nasa.gov/mfi/mag_cloud_pub1p.html). A strong geomagnetic storm (Dst = -300 nT, bottom plot) began at 1900 UT on July 15, 2000 and it was associated with an intense and prolonged southward magnetic field at the front edge of the magnetic cloud ($B_z = -44$ nT, second plot). This geomagnetic event was caused by a powerful CME, which first appeared in the field of view of the LASCO C2 instrument at 10:54 UT on July 14, 2000. The top right panel in Figure 1 shows a SOHO/LASCO C2 coronagraph image where the coronal ejecta is seen as a bright halo around the dark occulting disk (the white circle inside the disk marks the position and the apparent size of the solar disk). This halo CME originated in an active region NOAA 9077 located near the center of the solar disk. The 3B/5.7X “Bastille Day” flare (bottom panels in Figure 1) was associated with the ejecta. More details on this flare are discussed in elsewhere (e.g. *Aulanier et al., 2000; Zhang, et al., 2001; Yan et al., 2001; Yurchyshyn et al., 2001; Somov et al., 2002*).

In Figure 2 we plot the magnitude of B_z vs. the projected speed of the CME, V_p . The relationship between the projected speed of a CME and B_z (V_p-B_z) can be satisfactorily described by using the exponential function

$$B_z = 9.3 + 0.7 \exp(V_p/400), \quad (1)$$

where B_z is measured in nT and V_p is in kilometers per second. The solid line in the figure is the fit, while the dashed lines show the extent of the errors (rms = 7.3 nT). Figure 2 is evidence of the correlation between the speed of a CME and the B_z component of the IMF. The correlation coefficient is 0.78. Note that exclusion of the events with positive B_z does not noticeably change the correlation (0.77), although it significantly reduces the sample of events and thus decreases the reliability of the fit. Because of the lack of data for very fast CMEs ($V_p > 1200$ km/s), more extensive data set should be analyzed in order to make the V_p-B_z relationship more accurate.

4. Space Weather Application

Depending on the orientation of the magnetic field in an active region, and the sign of the magnetic helicity (magnetic twist), an

Table 1. List of earth directed CMEs

Date & Time of CME	V_p (km/s)	Date & Time of ICME	DoY	B_z nT
990413 03:30	290	990417 ^c 01:30	107	-14.3
990920 06:06	604	990922 21:00	265	-17.5
991018 02:06	1081	991021 04:00	294	+19.7
000118 17:54	739	000122 22:00	22	-15.2
000210 02:30	944	000212 01:00	43	-12.4
000404 16:21	1188	000406 20:00	97	-26.7
000714 10:54	1674	000715 ^c 19:00	197	-43.7
000809 16:30	702	000812 ^c 07:00	225	-28.1
000916 15:08	1215	000917 21:00	261	+23.8
001103 18:26	291	001107 ^c 01:00	312	-13.4
010409 15:54	1192	010411 ^c 20:00	101	-15.6
011025 15:26	1092	011028 03:00	301	-14.7
011104 16:35	1810	011106 02:00	310	-69.6
011122 20:30	1443	011124 09:00	328	+48.7

earthwardly directed CME may, or may not, have a southwardly directed magnetic component and, therefore, may, or may not, be associated with a geomagnetic storm. The key part is to establish if there is a southward component in the projected MC.

Yurchyshyn et al. [2001] analyzed two major flares and the associated CMEs. They found that directions of the helical magnetic fields in the leading edge of the magnetic clouds were consistent with the direction and helicity of the magnetic fields overlaying the active region filaments [see also *Bothmer and Schwenn 1994; Rust 1994; Marubashi 1997*]. The authors also concluded that the geoeffectiveness of CMEs with the NS oriented axial magnetic fields is mainly determined by this axial field, while in the case of CMEs with the EW oriented axial field, only the sign of magnetic helicity determines the sign of the z -component and thus the geoeffectiveness of a given CME.

Therefore, by using the methods described in *Yurchyshyn et al. [2001]*, we can predict the sign, and the orientation of the magnetic field in a halo CME, which originates close to the center of the solar disk. In the case when the magnetic field of the ICME was found to have a significant southward B_z component, its magnitude can then be estimated by equation (1). The projected speed of the halo CME can be determined in nearly real-time regime by measuring the position of the leading edge of a CME.

Further, the magnitude of the B_z component in sheath [*Cane et al. 2000*] and/or in magnetic clouds [*Wu and Lepping, 2002*] is found to be related to the intensity of a geomagnetic storm. The data, used in these studies was obtained by various satellites over the years 1965–1999. In order to be consistent with our study, which includes events from 1999–2001, we studied the B_z –Dst relationship by using ACE and Dst data for the same time interval. The number of events, is much larger than that used to study the V_p-B_z relationship. The reason for this is that we intended to study parameters of the solar wind only, we were no longer limited by the requirements described in previous section. Therefore, there was no need to identify the corresponding storm-related CME and its source region, which significantly increased the number of events suitable for the study. In Figure 3 we plot minimum values of the hourly averaged Dst index against minimum values of the B_z component (maximum negative values) for 72 events from 1998 to 2001 as measured by the ACE satellite. The solid line in Figure 3 is a third order polynomial fit to the data and is represented by

$$\text{Dst} = -2.846 + 6.54B_z - 0.118B_z^2 - 0.002B_z^3, \quad (2)$$

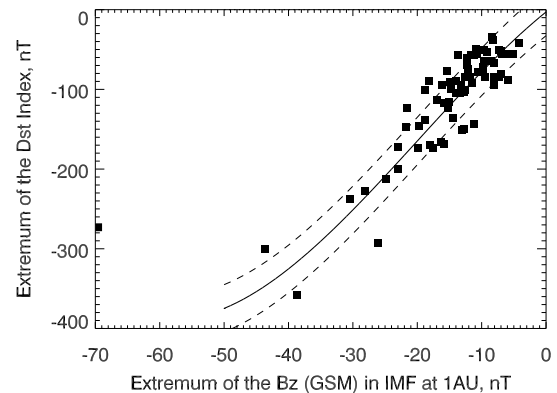


Figure 3. The intensity of geomagnetic storms (Dst) versus the strength of the southwardly directed magnetic field in an interplanetary ejecta (sheath and MCs). The solid line shows a polynomial fit and the dashed lines show the extent of the error to this fit.

where B_z and Dst are measured in nT. The dashed lines represent the extent of the error (rms = 30 nT). Note that, due to the limited data set, the fit is only reliable in the range $-40 \leq B_z \leq 0$ nT. This plot shows a strong B_z -Dst correlation, with a correlation coefficient of 0.82.

Since the southward IMF can be estimated immediately after the eruption based upon equation (1), the intensity of the geomagnetic storm can, therefore, be forecasted by using equation (2) at least one day in advance, assuming that the ejecta will encounter the earth's magnetosphere.

5. Concluding Remarks

Although the CME's projected speed appears to be one of the key parameters, which determine the magnitude of the IMF and thus the intensity of a storm, the duration of the southward directed B_z , and the parameters of the solar wind, such as velocity and density, also contribute to a storm. All of these most probably cause the significant scatter in the V_p - B_z plot and it impose certain limitations on the accuracy of the predictions in the case of slow ($V_p < 1200$ km/s) CMEs. Thus, based on Figures 2 and 3 we can conclude that CMEs with speeds of 1200 km/s or less are responsible for storms with a Dst index > -200 nT. Meanwhile, very fast CMEs ($V_p > 1200$ km/s) are capable of causing extremely intense storms, when the Dst index decreases below -300 nT. Taking into account possible uncertainties we further conclude that the described approach is able to estimate the upper bound of the field intensity and, therefore, the upper bound of the Dst index. Further progress in our understanding of propagation of a CME in the interplanetary space may improve accuracy of the predictions of intense geomagnetic storms.

In summary, we would like to organize the main conclusions as follows.

1) We found a high correlation (coefficient 0.78) between the hourly averaged ACE measurements of the B_z component of the interplanetary magnetic field and the projected speeds of 14 halo CMEs, that originate from the central part of the solar disk ($R < 0.8R_\odot$). The association between the CME speeds and the magnitude of IMF is most pronounced for very fast CMEs while it is less apparent in the case of slow ejecta.

2) Study of the relationship between the magnitude of the southward IMF and the Dst index supports earlier reports: the hourly averaged B_z , measured in the GSM system are correlated with the hourly averaged Dst index.

3) Findings, presented here, suggest that CMEs with speeds of 1200 km/s or less are responsible for storms with a Dst index > -200 nT, while the high speed CMEs ($V_p > 1200$ km/s) are capable of causing extremely intense storms.

Acknowledgments.

We are much obliged to referees whose constructive criticism led to significant improvement of the manuscript. We are also grateful to T. J. Spirock for careful proofreading. We thank the ACE MAG instrument team and the ACE Science Center for providing the ACE data. We acknowledge the use of geomagnetic data from the World Data Center for Geomagnetism in Kyoto. The CME catalog is generated, and maintained, by the Center for Solar Physics and Space Weather, The Catholic University of America in cooperation with the Naval Research Laboratory and NASA. SOHO is a project of international cooperation between ESA and NASA. This work was supported, in part, by ATM-9903515, ATM-0205157, ATM-0076602 and NASA(NAG5-9682) grants.

References

Aulanier, G., E.E. DeLuca, S.K. Antiochos, R.A. McMullen, L. and Golub, The Topology and Evolution of the Bastille Day Flare, *Astrophys. J.*, 540, 1126, 2000.

Bothmer, V., and R. Schwenn, Eruptive prominences as sources of magnetic clouds in the solar wind, *Space Sci. Rev.*, 70, 215, 1994.

Burlaga, L. F., E. Sittler, F. Mariani, and R. Schwenn, Magnetic loop behind an interplanetary shock - Voyager, Helios, and IMP 8 observations, *J. Geophys. Res.*, 86, 6673, 1981.

Burton, R.K., R.L. McPherron, and C.T. Russell, An empirical relationship between interplanetary conditions and Dst, *J. Geophys. Res.*, 80, 4204, 1975.

Canfield, R.C., H.S. Hudson, and D.E. McKenzie, Sigmoidal morphology and eruptive solar activity, *Geophys. Res. Lett.*, 26, 627, 1999.

Cane, H.V., I.G. Richardson, and O.C. St. Cyr, Coronal mass ejections interplanetary ejecta and geomagnetic storms, *Geophys. Res. Lett.*, 27, 3591, 2000.

Fenrich, F.R., and J.G. Luhmann, Geomagnetic response to magnetic clouds of different polarity, *Geophys. Res. Lett.*, 25, 2999, 1998.

Gonzalez, W.D., and B.T. Tsurutani, Criteria of interplanetary parameters causing intense magnetic storms (Dst < -100 nT), *Planet Space Sci.*, 35, 1101, 1987.

Gonzalez, W.D., J.A. Joselyn, Y. Kamide, H.W. Kroehl, G. Rostoker, B.T. Tsurutani, and V.M. Vasyliunas, What is a geomagnetic storm? *J. Geophys. Res.*, 99, 5771, 1994.

Gosling, J.T., E. Hildner, R.M. MacQueen, R.H. Munro, A.I. Poland, and C.L. Ross, Mass ejections from the sun - A view from SKYLAB, *Astrophys. J.*, 79, 4581, 1974.

Howard, R. A., D.J. Michels, N.R. Sheeley Jr, and M.J. Koomen, The observation of a coronal transient directed at earth, *Astrophys. J.*, 263, L101, 1982.

Lindsay, G.M., J.G. Luhmann, C.T. Russell, and J.T. Gosling, Relationship between coronal mass ejection speeds from coronagraph images and interplanetary characteristics of associated interplanetary coronal mass ejections, *J. Geophys. Res.*, 104, 12515, 1999.

Low, B.C., Coronal Mass ejections, magnetic flux ropes, and solar magnetism, *J. Geophys. Res.*, 106, 25141, 2001.

MacQueen, R. M., J. A. Eddy, J.T. Gosling, E. Hildner, R.H. Munro, G.A. Jr Newkirk, A.I. Poland, and C.I. Ross, The Outer Solar Corona as Observed from Skylab: Preliminary Results, *Astrophys. J.*, 187, L85, 1974.

Marubashi, K., Interplanetary Magnetic Flux Ropes and Solar Filaments, in *Coronal Mass Ejections, Geophysical Monograph 99*, ed. N. Crooker, J.A. Joselyn, and J. Feynman (Washington, DC: AGU), 147, 1997.

Pevtsov, A.A., and R.C. Canfield, Solar magnetic fields and geomagnetic events, *J. Geophys. Res.*, 106, 25191, 2001.

Rostoker, G. and C.-G. Fälthammar, Relationship between changes in the interplanetary magnetic field and variations in the magnetic field at the Earth's surface, *J. Geophys. Res.*, 72, 5853, 1967.

Russell, C.T., R.L. McPherron, and R.K. Burton, On the cause of geomagnetic storms, *J. Geophys. Res.*, 79, 1105, 1974.

Rust, D.M., Spawning and shedding helical magnetic fields in the solar atmosphere, *Geophys. Res. Lett.*, 21, 241, 1994.

Shanmugaraju, A., Y.-J. Moon, M. Dryer, and S. Umapathy, On the kinetic evolution of flare-associated CMEs, *Sol. Phys.*, 215, 185, 2003.

Sheeley, N.R.Jr., J.H. Walters, Y.-M. Wang, and R.A. Howard, Continuous tracking of coronal outflows: two kinds of coronal mass ejections, *J. Geophys. Res.*, 104, 24739, 1999.

Schwenn, R., A. Dal Lago, W. D. Gonzalez, E. Huttunen, C. O. St. Cyr, and S. P. Plunkett, A tool for improved space weather predictions: the CME expansion speed, *Eos Trans.*, 82, 47, AGU Fall Meet. Suppl., Abstract SH12A-0739, 2001.

Somov, B. V., T. Kosugi, H.S. Hudson, T. Sakao, and S. Masuda, Magnetic reconnection scenario of the Bastille Day 2000 flare, *Astrophys. J.*, 579, 863, 2002.

Tousey, R., The solar corona, in *COSPAR Space Research, XIII*, 713, 1973.

Zhang, J., J. Wang, Y. Deng, and D. Wu, Magnetic Flux Cancellation Associated with the Major Solar Event on 2000 July 14, *Astrophys. J.*, 548, L99, 2001.

Wilson, R.M., and E. Hildner, E., Are interplanetary magnetic clouds manifestations of coronal transients at 1 AU? *Solar Phys.*, 91, 169, 1984.

Wu, C.C., and R.P. Lepping, The effect of solar wind velocity on magnetic cloud-associated magnetic storm intensity, *J. Geophys. Res.*, 107, A11, 1346, 2002.

Yan, Y., Y. Deng, M. Karlick, Q. Fu, S. Wang, and Y. Liu, The Magnetic Rope Structure and Associated Energetic Processes in the 2000 July 14 Solar Flare, *Astrophys. J.*, 551, L115, 2001.

Yurchyshyn, V.B., H. Wang, P.R. Goode, and Y. Deng, Orientation of the Magnetic Fields in Interplanetary Flux Ropes and Solar Filaments, *Astrophys. J.*, 563, 381, 2001.

(Received _____)